Proceedings of the 4th International Conference on Fluid Flow and Thermal Science (ICFFTS'23)
Lisbon, Portugal- December 07 - 09, 2023
Paper No. 163
DOI: 10.11159/icffts23.163

Curvature Effect on Fouling and Heat Transfer of a Thick Curved Plate

Li Hongying[1], MD Didarul Islam[2], Afshin Goharzadeh[2], Yap Yit Fatt[2*]
[1]A*STAR Institute of High Performance Computing,
1 Fusionopolis Way, Connexis, 138632, Singapore
lih@ihpc.a-star.edu.sg;
[2]Department of Mechanical Engineering, Khalifa University,
127788, Abu Dhabi UAE
didarul.islam@ku.ac.ae; afshin.goharzadeh@ku.ac.ae; *yap.fatt@ku.ac.ae

Abstract - Fouling and heat transfer on a plate depends strongly on the plate geometry. The present study assesses the influence of plate curvature on fouling (combined particle deposition and deposit erosion) and heat transfer on a thick curved plate with volumetric heat generation under cross-flow configuration. Convex, concave and flat plates are considered for three different plate orientations: parallel $0°$, inclined $45°$ and perpendicular $90°$ to the flow. A numerical model with flow, heat transfer, particle transport, particle deposition and deposit erosion fully-coupled is employed. It is found that the amount of deposit formed generally increases with the projected blockage area of the plate with a thicker deposit layer on the upstream facing plate surface, deposit erosion is dominant in the upper and lower flow passages, and exposed tip or plate surface, i.e. not covered by deposit, is the most important in dissipating the heat within the plate to the adjacent flowing fluid.

***Keywords*:** fouling, heat transfer, curved plate, particle deposition, deposit erosion

1. Introduction

Heat transfer with fouling occurring at the same time is encountered in many engineering applications including cross-flow heat exchangers. Fouling affect negatively the heat transfer performance as the insulating deposit layer obstruct heat flow and at the same time increasingly blocking the flow passages leading to higher pressure drop. Fouling is generally a net effect of particle deposition (increase deposit) and deposition erosion (remove deposit) driven by for example shear stress. Fouling has been studied extensively including for tube bundle heat exchangers [1], fin-and-tube heat exchangers [2], ventilation ducts [3] and slit microchannel [4], and still not well understood fundamentally given the complex interacting phenomena of fluid flow, heat transfer, particle transport, particle deposition and deposit erosion occurring simultaneously. Fundamental understanding can be easier derived from simpler geometry, e.g. flat plate. Fouling and heat transfer on a flat plate was investigated numerically in our earlier study [5]. Here in this study, the work is extended to assess the influence of plate curvature on fouling and heat transfer.

2. Mathematical Model

Figure 1 shows a channel of length L_o and height H_o containing a thick curved plate at the center. The plate with length $\tilde{l}$, thickness h and sign radius R is oriented with an angle β to the flow direction. The sign radius R is defined such that $R=+ve$, $R=-ve$ and $R=\infty$ correspond respectively to convex (shown in Fig. 1), concave and flat plates. The upper and lower channel walls are thermally insulated. Initially, the quiescent fluid and the plate are at temperature T_o. At time $t=0^+$, fluid flows into the channel at the inlet at velocity u_o, temperature T_o and particle concentration C_o. At the same time, the plate starts to generate heat with a volumetric heat generation of $\dot{q}_{gen}$. The flowing fluid carries the generated heat away, cooling the plate in the process. The particles suspended in the fluid driven convectively and diffusively towards the plate where particle deposition occurs forming a growing deposit layer around the plate. Shear stress generated by the flowing fluid at the same time erodes the deposit layer. Heat is now required to be transferred from the plate to the fluid across the insulating deposit layer, and as a result, heat transfer deteriorates leading to a higher temperature within the plate. Fluid with a lower particle concentration but at a higher temperature flows out of the channel at the outlet.

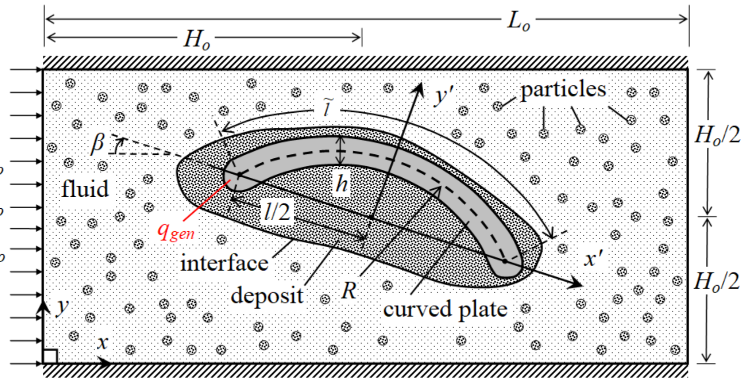

Figure 1: Schematic of a curve plate in a channel.

The transports of fluid, momentum, particles and energy in the channel are governed by

$$\nabla^* \bullet \vec{u}^* = 0 \tag{1}$$

$$\frac{\partial(\rho^* \vec{u}^*)}{\partial t^*} + \nabla^* \bullet (\rho^* \vec{u}^* \vec{u}^*) = -\nabla^* p^* + \nabla^* \bullet \left[\frac{\mu^*}{\mathrm{Re}} \left(\nabla^* \vec{u}^* + \nabla^* \vec{u}^{*T} \right) \right] \tag{2}$$

$$\frac{\partial C^*}{\partial t^*} + \nabla^* \bullet (\vec{u}^* C^*) = \nabla^* \bullet \left(\frac{D^*}{Pe_C} \nabla^* C^* \right) - DaC^* \delta^*(\phi) |\nabla \phi| \tag{3}$$

$$\frac{\partial [(\rho c)^* T^*]}{\partial t^*} + \nabla^* \bullet [(\rho c)^* \vec{u}^* T^*] = \nabla^* \bullet \left(\frac{k^*}{Pe_T} \nabla^* T^* \right) + S^* \tag{4}$$

where dimensionless velocity $\vec{u}^* = \vec{u} / u_o$, dimensionless pressure $p^* = p / \rho_f u_o^2$, dimensionless temperature $T^* = \rho_f c_f u_o (T - T_o) / \dot{q}_{gen} H_o$ and dimensionless particle concentration $C^* = C / C_o$ are defined. The fluid-deposit interface evolves over time. The movement of interface is captured using a narrow-band level-set approach. The level-set function ϕ is driven by the interfacial velocity $\vec{u}_\Gamma^*$ given by

$$\vec{u}_\Gamma^* = DaC_o^* C_\Gamma^* \hat{n}_\Gamma - \frac{Er}{\rho_d^*} \max \left\langle (|\tau_\Gamma^*| - \tau_{crit}^*), 0 \right\rangle \hat{n}_\Gamma \tag{5}$$

In Eq. (5), the first and second terms are attributed respectively to particle deposition and shear driven deposit erosion.

Essentially, the transport processes are characterized by the following dimensionless numbers. *Geometrical*: $L_o^* = L_o / H_o$, $\tilde{l}^* = \tilde{l} / H_o$, $h^* = h / H_o$, β and curvature ratio $CR = sign(R) \dfrac{\tilde{l} - l}{l(\pi/2 - 1)}$. Note that $CR = +1$, $CR = 0$ and $CR = -1$ correspond respectively to semi-circular convex, semi-circular concave and flat plates. *Properties*: dimensionless deposit and plate densities ($\rho_d^* = \rho_d / \rho_f$ and $\rho_p^* = \rho_p / \rho_f$), dimensionless deposit and plate volumetric heat capacities ($(\rho c)_d^* = (\rho c)_d / (\rho c)_f$ and $(\rho c)_p^* = (\rho c)_p / (\rho c)_f$) and dimensionless deposit and plate thermal diffusivities ($\alpha_d^* = \alpha_d / \alpha_f$ and $\alpha_p^* = \alpha_p / \alpha_f$). *Physical*: Reynolds number $\mathrm{Re} = \rho_f u_o H_o / \mu_f$, particle Peclet number $Pe_C = u_o H_o / D_C$, Damkholer number $Da = \tilde{k}_d / u_o$, thermal Peclet number $Pe_T = u_o H_o / \alpha_f$, dimensionless inlet particle concentration $C_o^* = C_o / \rho_d$, erosion number $Er = \tilde{k}_{er} u_o$ and dimensionless critical shear stress $\tau_{crit}^* = \tau_{crit} / \rho_f u_o^2$. The subscripts f, d and p refer to quantities associated respectively to the fluid, deposit and plate. The solution procedure is documented in [0] and will not be repeated here. To quantify the amount of deposit accumulated over time, the dimensionless deposit volume $V_d^*(t^*) = V_d(t) / V_f\big|_{t=0}$ where V_d and V_f are respectively the deposit and fluid volumes in the channel is introduced.

3. Results and Discussions

The model was validated in our earlier studies [6-7] and therefore will not be repeated here. The governing dimensionless parameters are set to: (geometrical) $L_o^* = L_o / H_o$, $\tilde{l}^* = 0.5$, $h^* = 0.05$, $\beta = 45°$, (properties) $\rho_d^* = 10$, $\rho_p^* = 1$, $(\rho c)_d^* = 1$, $(\rho c)_p^* = 1$, $\alpha_d^* = 0.1$, $\alpha_p^* = 10$ and (physical) $\mathrm{Re} = 1$, $Pe_C = 15$, $Da = 0.667$, $Pe_T = 1$, $C_o^* = 0.1$, $Er = 0.005$, $\tau_{crit}^* = 0$. As the curvature effect is of interest, it is varied as $CR = +1$, $+0.3665$, $+0.0827$, 0, -0.0827, -0.3665, -1. Figure 2 shows the mesh independent solutions with $\vec{u}^*$, C^* and T^* plotted at $t^* = 10$. The fluid-deposit interface captured by ϕ starting from $t^* = 0$ up to $t^* = 9$ is superimposed as well. The deposit morphology depends strongly on CR, i.e. the curvature effect. Overall, the deposit layer is thicker on the upstream facing surface of the plate and thinner on the downstream facing surface. This is attributed to a higher particle concentration in the upstream, resulting in higher deposition rate. As particles are consumed, the particle concentration downstream is therefore lower.

For the cases of $CR = +1$ and $CR = -1$, the region adjacent to the concave surface has a significantly thinner deposit layer. Particles rely mainly on convection to be transported towards the fluid-deposit interface, but mainly diffusion from there onto the fluid-deposit interface where deposition actually occurs. Constrained by the geometrical features of an increasingly close region, convection can no longer transport particles into this region, and diffusion is too slow to replenish the deposited particles in the region. Therefore, the deposit layer grows very slowly.

Shear erosion dominantly affects the deposit layer growth in the upper region. The deposit layer could not grow thicker towards the upper wall (resulting in a flat fluid-deposit interface) as further growth would results in a narrower flow passage, generating higher shear stress and therefore eroding any additionally formed deposit. This occurs to a certain extent to the lower region for the cases of $CR = -0.0827$, -0.3665 and -1. There is no deposit formed at the tips of the plate (except the upper tip for the cases of $CR = +1$ and $+0.3665$) attributed to strong local shear driven deposit erosion.

The dimensionless deposit volume V_d^* and dimensionless average temperature T_{ave}^* over time are plotted in Fig. 3. The amount of deposit formed relates closely with (1) the projected blockage area to the flow (allow more particles to impact and deposit on surface for deposition and lesser shear driven erosion on the upper and lower part of the deposit formed) and (2) whether the plate is curved towards upstream (as in the cases of $CR = -ve$, where there is a higher particle concentration of the incoming fluid leading to higher deposition rate). Within the range of $CR = 0$ to $CR = -1$, V_d^* increases with a higher $|CR|$ as the projected blockage area is higher. The cases of $CR = +1$ and $CR = +0.3665$ are special, as the projected blockage area increases over time during the deposition process. The projected blockage area for these cases approaches that of the case $CR = +0.0827$. For the range of $CR = +1$ to $CR = 0$, the trend of V_d^* as CR decreases is not monotonic as now factors (1) and (2) compete with each other. The effect of factor (2) in influencing V_d^* can be concluded by careful examination of the cases of $CR = +0.0827$ (plate curved towards downstream) and $CR = -0.0827$ (plate curved towards upstream) with the case of $CR = -0.0827$ having larger V_d^*.

Effectiveness in heat removal from the plate can be compared through the plate temperature. Note that for the cases of $CR = +1$ and $+0.3665$, the region near the upper tips (fully covered by deposit) has a higher temperature. For these cases, the plate temperature decreases towards the lower tips (exposed to fluid). Given the insulating effect of the deposit layer, heat generated in the plate is conducted towards to lower tips for transfer to the fluid. Any exposed plate surface then plays similar role. From Fig. 3, T_{ave}^* for these cases is highest. For all other cases, both tips are exposed ($CR = +0.0827$,

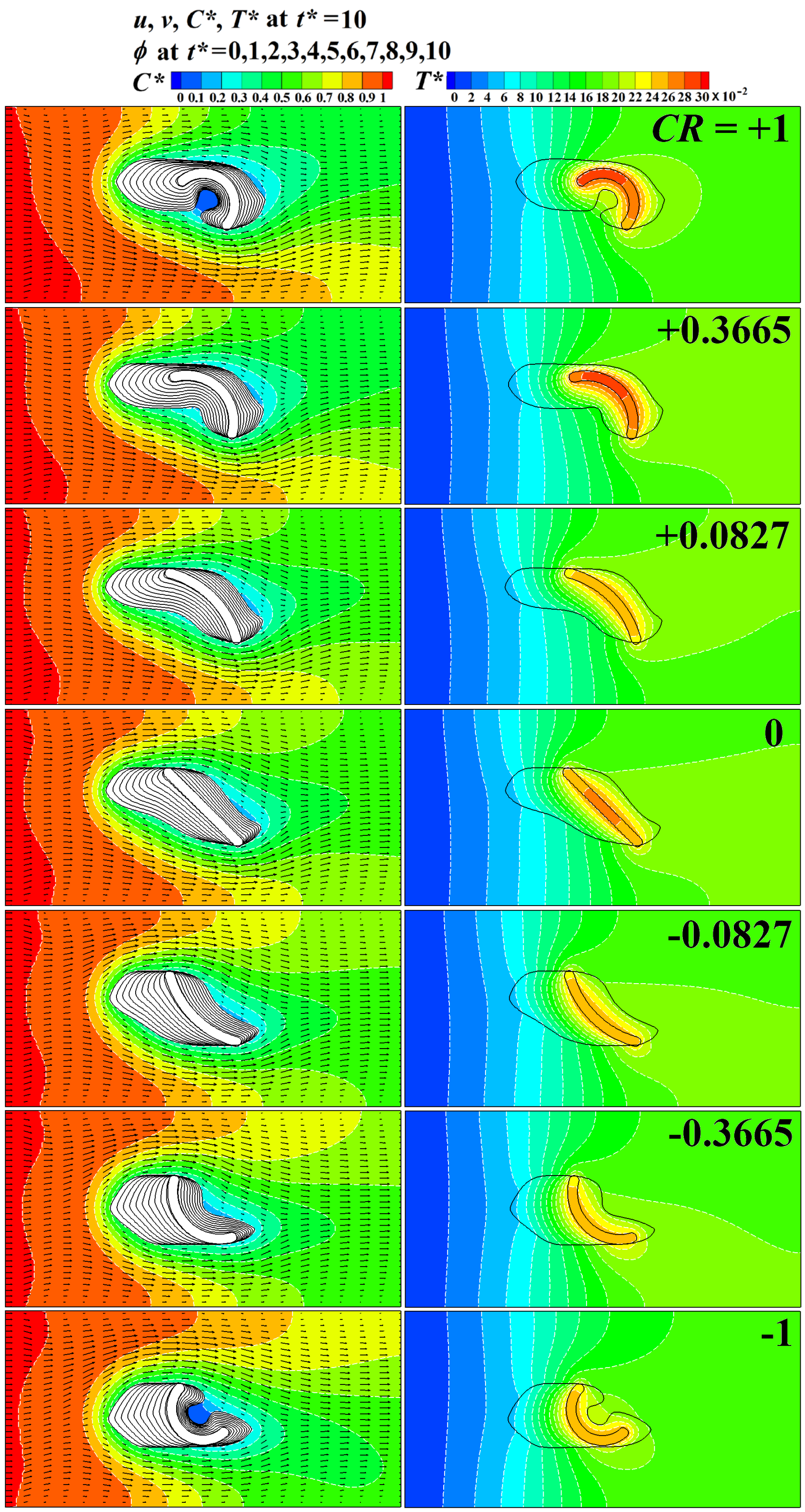

Figure 2: Effect of CR on deposition on curved plates with $\beta = 0°$.

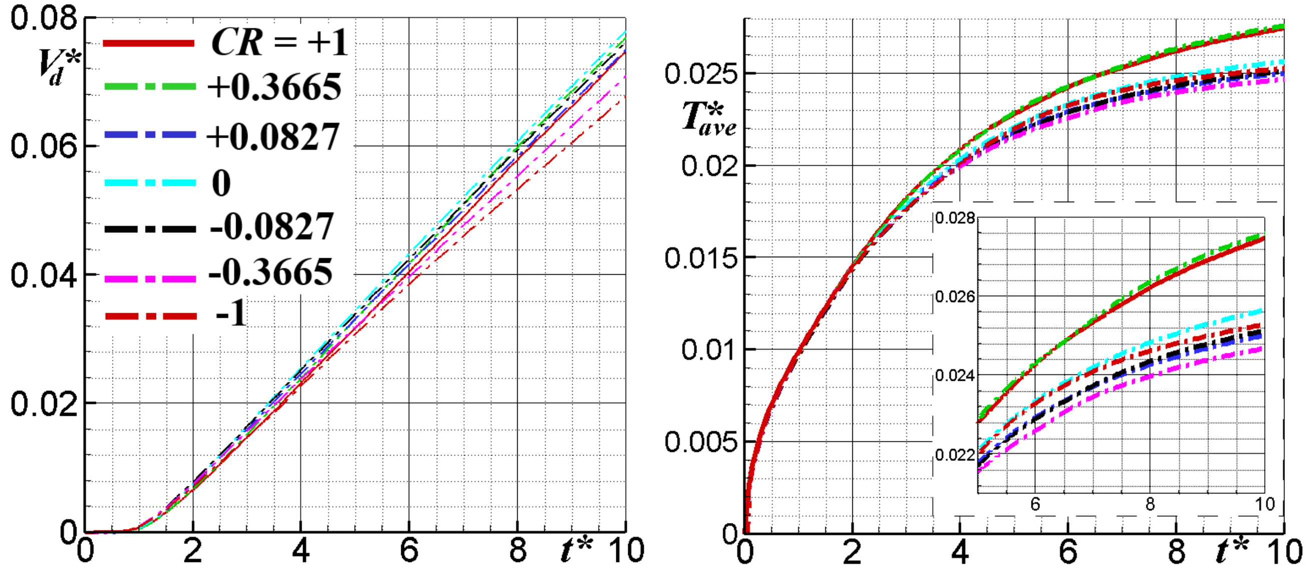

Figure 3: V_d^* and T_{ave}^* for curved plates with $\beta = 0°$.

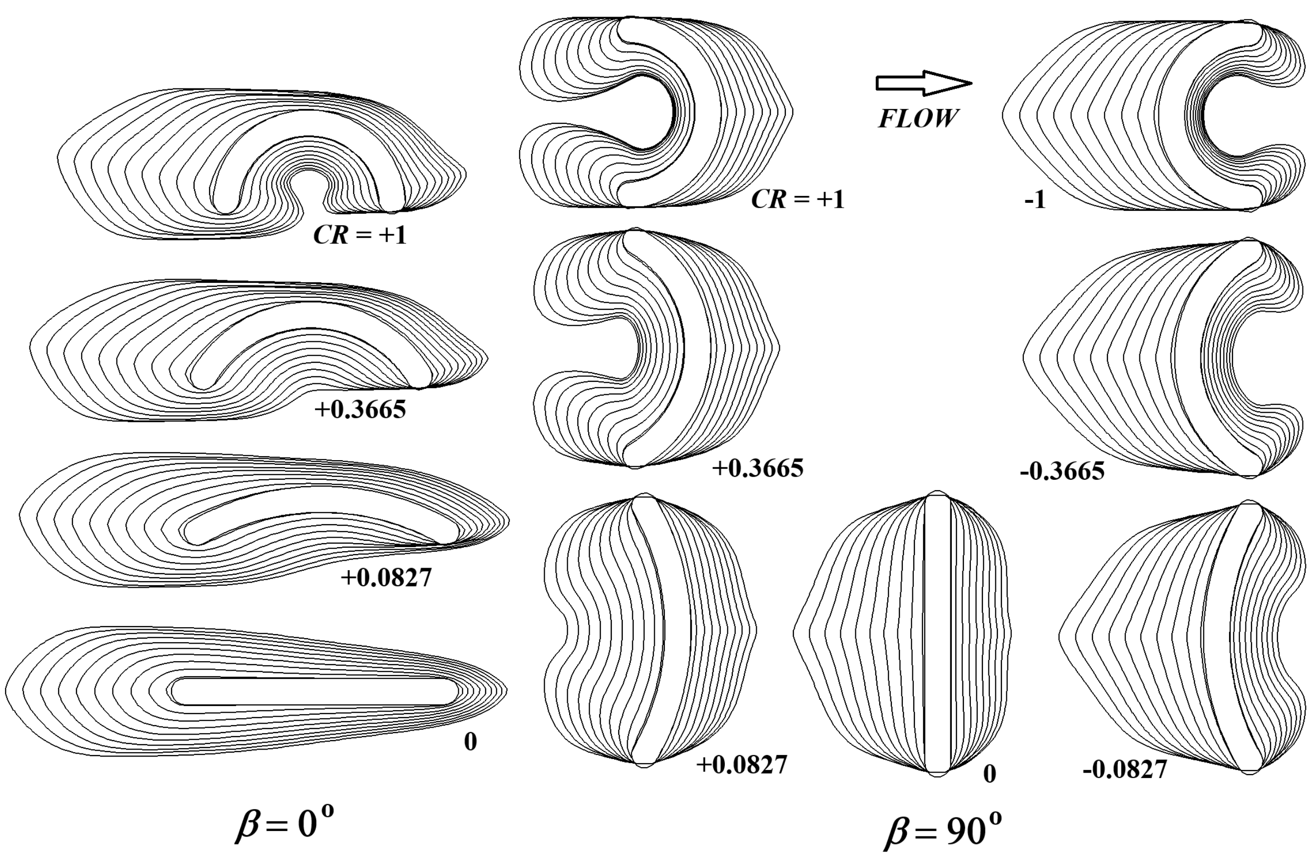

Figure 4: Effect of CR on curved plates with $\beta = 0°$ and $\beta = 90°$.

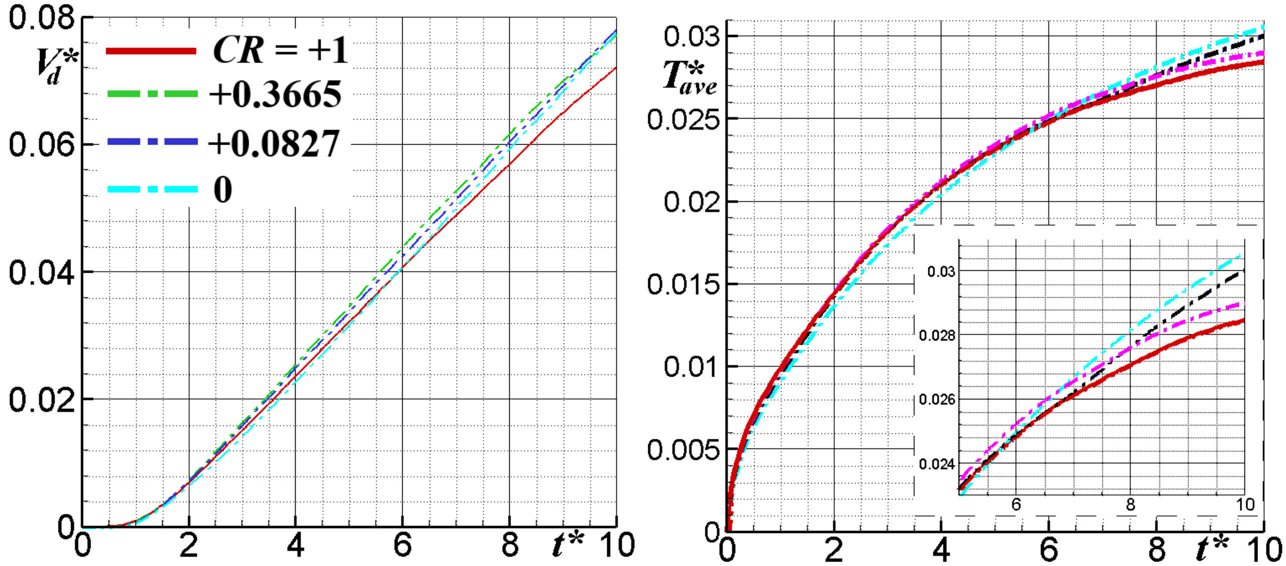

Figure 5: V_d^* and T_{ave}^* for curved plates with $\beta = 0°$.

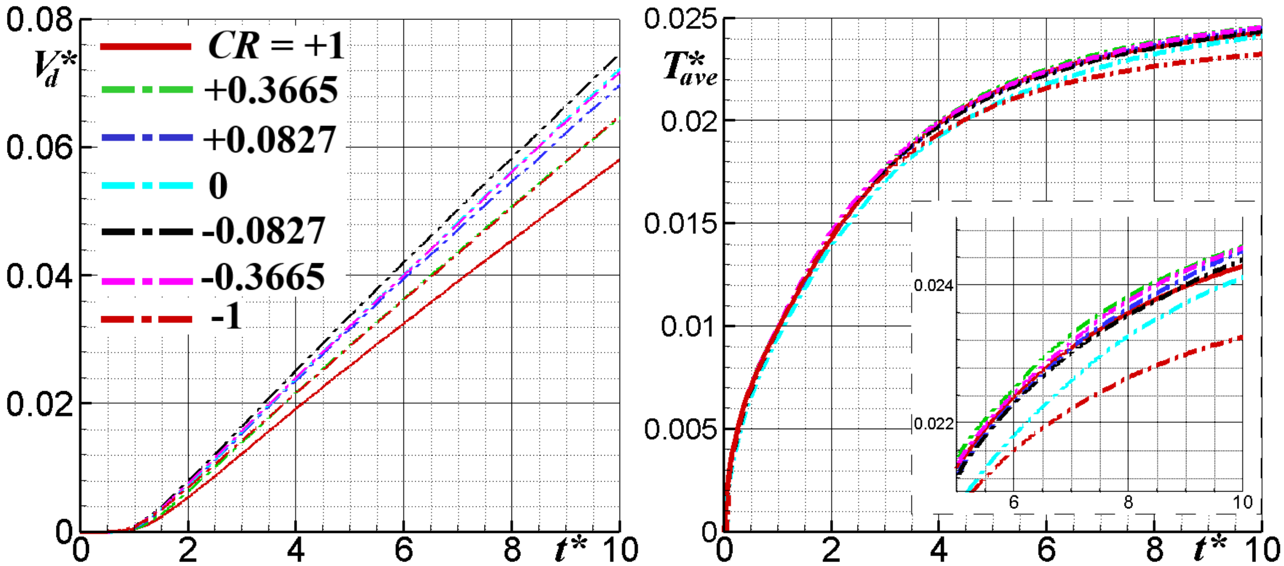

Figure 5: V_d^* and T_{ave}^* for curved plates with $\beta = 90°$.

0, -0.0827) and upper tips plus part of the lower convex surface exposed ($CR = -0.3665$, -1), hence the curved plate has a noticeable lower temperature. The substantial decreases in T_{ave}^* from the case of $CR = +0.3665$ (one tip exposed) to the case of $CR = +0.0827$ (both tips exposed) exemplified role exposed tip in augmenting heat transfer.

Figure 4 shows the deposit morphology for plate oriented with $\beta = 0°$ and $\beta = 90°$. Figure 5 and 6 shows the plots of V_d^* and T_{ave}^* respective for $\beta = 0°$ and $\beta = 90°$. For $\beta = 0°$, the projected blockage area increases with time for all CR and the highest plate temperature is found for the case of $CR = 0$ with the plate completely covered by the deposit layer. For $\beta = 0°$, note that for a given CR, the projected blockage area does not change with time. For the range of

$CR=+1$ to $CR=0$, V_d^* increases for the case of lower CR, i.e. larger projected blockage area. For the range of $CR=-1$ to $CR=-0.0827$, V_d^* increases for the case of lower $|CR|$ for the same reason. The effect of factor (2), i.e. whether the plate is curved towards upstream or downstream, on V_d^* can be best exemplified by comparison of $CR=+1$ and $CR=-1$ or $CR=+0.0827$ and $CR=-0.0827$.

In terms of heat transfer, the cases of $CR=+1$ and $CR=-1$ are interesting in comparison. The plots of $\vec{u}^*$, C^* and T^* at $t^*=10$ for these cases are shown in Fig. 7. The case of $CR=+1$ has a higher T_{ave}^* than that for the case of $CR=-1$. In these two cases, both tips are exposed to the flowing fluid. However, in the case of $CR=-1$, the flow starts to expand upon passing the tips, effectively taking more heat with it.

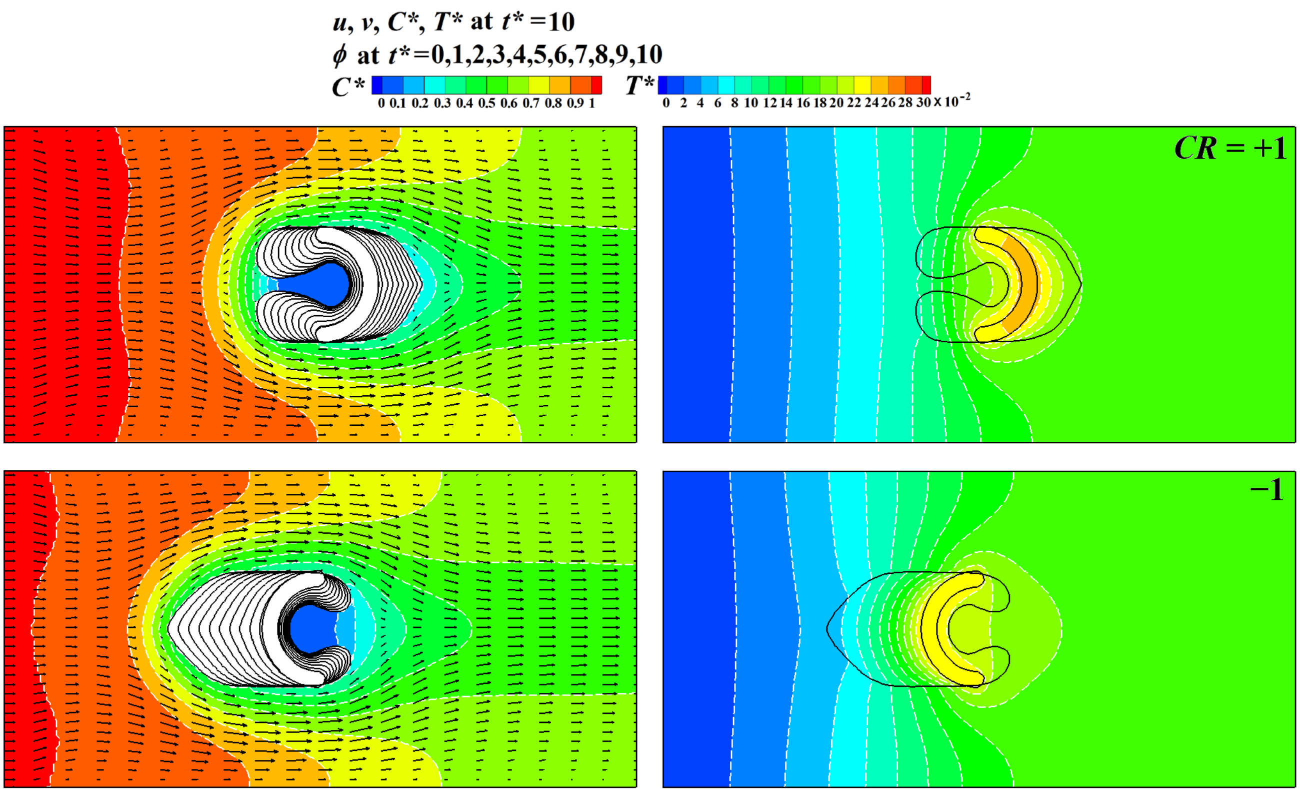

Figure 7: Effect of CR on deposition on curved plates with $\beta=90°$.

4. Conclusion

The current studies investigated the effect of curvature (quantified by CR) of a curved plate on particle deposition, deposit erosion and heat transfer under a cross flow configuration. The deposit morphology is strongly affected by CR. The amount of deposit formed generally increases with projected blockage area of the plate, then, to certain extent when the plate is curved towards upstream. Deposit erosion is particular strong adjacent in upper and lower flow passages, resulting in a relative flat fluid-deposit interface. Under the insulating effect of the deposit layer, exposed tip or plate surface contributes substantially in removing the generated heat in the plate to the flowing fluid. These observations provide additional understanding in designing proper fin geometry on cross-flow heat exchangers.

References

[1] S.-Z. Tang, F.-L. Wang, Q. Ren and Y.-L. He, "Fouling characteristics analysis and morphology prediction of heat exchangers with a particulate fouling model considering deposition and removal mechanisms," *Fuel*, vol. 203, pp. 725-738, 2017.

[2] T. Välikangas, J. Hærvig, H. Kuuluvainen, M.D. Maso, P. Peltonen and V. Vuorinen, "Deposition of dry particles on a fin-and-tube heat exchanger by a coupled soft-sphere DEM and CFD," *Int. J. Heat Mass Tran.*, vol. 149, pp. 119046, 2020.

[3] Z. Han, Z. Xu and X. Yu, "CFD modeling for prediction of particulate fouling of heat transfer surface in turbulent flow," *Int. J. Heat Mass Tran.*, vol. 144, pp. 118428, 2019.

[4] M. Trofa, G. D'Avino, L. Sicignano, G. Tomaiuolo, F. Greco, P.L. Maffettone and S. Guido, "CFD-DEM simulations of particulate fouling in microchannels," *Chem. Eng. J.*, vol. 358, pp. 91-100, 2019.

[5] Li H., MD.D. Islam, A. Goharzadeh and Yap Y.F., "Fouling on an Inclined Thick Flat Plate in a Channel," in *13th International Conference on Thermofluids*, Yogyakarta, Indonesia, 25-26th Oct. 2022, Paper 1570837341.

[6] Yap Y.F., F.M. Vargas and J.C. Chai, "A level-set method for convective-diffusive particle deposition," *Appl. Math. Model.*, vol. 37, pp. 5245-5259, 2013.

[7] Guan Q., Li H., A. Goharzadeh, MD.D. Islam, Kang C.W. and Yap Y.F., "Laminar Cross-Flow Convective Heat Transfer of a Finned Cylindrical Tube in the Presence of Particle Deposition and Deposit Erosion," Appl. Therm. Eng., in press.